Thermal Buckling Study of Empty Thin-Walled Steel Tanks Due To Fire Scenarios

Bian Rui, Pan Ke

Abstract— In order to reduce the failure probability of the storage tank under thermal radiation conditions, this paper aims to study the post-thermal buckling behavior of fixed headspace thin steel storage tanks under thermal radiation. Finite element software ABAQUS was used to simulate the key factors affecting the thermal buckling response of the target tank (flame height, wind speed, and tank diameter). The results show that the deformation of the tank is directly proportional to the flame height, wind speed and tank diameter. The degree of depression deformation of the target tank will increase with the increase in flame height. The existence of wind speed increases the radial displacement amplitude of the tank wall, and the degree of unevenness of the wall intensifies. Compared with D=5, the deformation degree of the tank and the number of post-buckling occurred more frequently and more intensely in D=10. The reasonable layout of the storage tank position can increase the refractory time of the storage tank, and increase the minimum critical buckling temperature to prevent the occurrence of buckling behavior after heat.

Index Terms— Thermal radiation, thermal buckling, ABAQUS, hollow thin-walled steel tank

I. INTRODUCTION

With the booming development of the petrochemical industry, the number of storage tanks has been increasing, and their volumes have been growing larger. The oil products stored in these tanks are often flammable and explosive, while ignition sources such as lightning, static electricity, and various open flames can potentially trigger tank fires. Therefore, tank fires are one of the most common accidents in tank farms^[1]. On April 6, 2015, a leak and fire occurred in the paraxylene unit of Zhang zhou Gu lei Teng long Aromatics, igniting two heavy oil storage tanks and one light reformate storage tank in the intermediate tank farm. The fire was extinguished and reignited twice. During the second reignition, two fire trucks were destroyed, ultimately leading to the rupture and ignition of the neighboring non-accident tank 609. Meanwhile, the top of the slightly distant tank 202 showed partial deformation, with a tendency to rupture and ignite. The spread of fires in tank groups involves the fire dynamics evolution of the ignited tank, the process of radiative heat transfer, and the thermal response and failure characteristics of adjacent non-accident tanks [2]. Therefore, studying the radiative heat transfer process in pool fires is of significant practical importance.

The tank walls of steel storage tanks are usually very thin, and thermal buckling is the main failure mode under

Manuscript received October 10, 2025

Bian Rui, School of traffic Engineering, Dalian Jiaotong University, Dalian, Liaoning 116028, China.

Pan Ke*, corresponding author, School of traffic Engineering, Dalian Jiaotong University, Dalian, Liaoning 116028, China

thermal loading, Salahshour S et al. studied the thermal buckling behavior of steel cylindrical shells and storage tanks under fire [3]. A large number of studies have been published in this area. Pantousa D proposes some mathematical expressions to describe and simulate the buckling behavior of pool fires on storage tanks [4]. In addition, Li et al. investigated the effects of pool fires on adjacent storage tanks, the thermal response of liquids stored in these tanks, and the possibility of fire escalation [5-6]. However, the above study ignored the effect of the spacing between the fire tank and the adjacent heated tank on heat transfer. Therefore, Rossana C Jaca et al. assumed that the pool fire flame is a solid flame and the temperature of the flame surface is uniformly distributed and constant, and established a finite element model to predict the temperature distribution of adjacent tanks under the action of thermal radiation of a fire tank using the cavity radiation model, and studied the thermal buckling behavior of steel storage tanks under the action of thermal radiation of fire tanks [7-8].

At present, the fire spacing of oil storage tanks in our country is based on past historical accident data and is formulated on the basis of experience. Although the thermal radiation damage model is used to predict the fire scene and the thermal radiation intensity of the adjacent storage tank is obtained, there is a lack of discussion on the thermal response results of the storage tank under the nonlinear distribution of thermal radiation intensity, and the basis for formulating the fire protection spacing is incomplete.

Therefore, Abaqus software is used to establish a finite element model for the failure analysis of fixed vault steel tanks under the action of heat radiation by different factors. Firstly, the thermal buckling response of the storage tank under the action of thermal radiation at different flame heights was studied. Secondly, the effect of flame on the fire resistance of the target tank under different wind speeds is studied, and finally the effect of different tank diameters on the fire resistance of the tank is studied. The failure mechanism of the storage tank was studied by analyzing the stress change process of the tank wall.

II. MODEL BUILDING

A. Tank model

The target tank is designed according to the national table GB-50341-2014, with a diameter of 20 m, a tank wall height of 17.82 m, and an overall height of 20 m ^[9]. The overall size of the target tank is 200mm using the unencrypted grid division method, and the grid division is shown in Fig.1. The thermal buckling analysis was performed using the display kinetics method, and the cell type of the target tank was S4R.

Thermal Buckling Study of Empty Thin-Walled Steel Tanks Due To Fire Scenarios

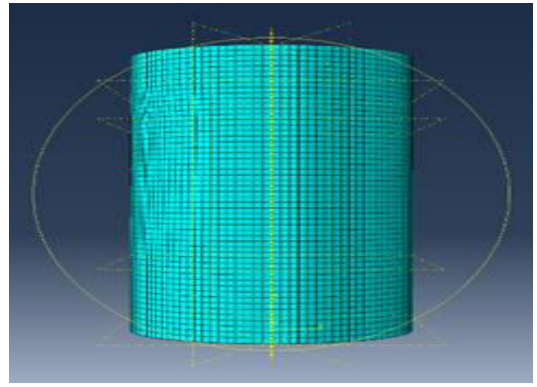


Figure 1 Meshing of the target tank

B. Flame model

Pool fire is defined as the turbulent diffusion of a burning flame over a horizontal pool of evaporated hydrocarbon fuel. Fuels can be liquid, gas, or solid. There are a wide variety of mathematical expressions used to predict the behavior of hydrocarbon pool fires, varying from field models (also known as computational fluid dynamics, or CFD models) to empirical (or semi-empirical models).

Empirical models are based on dimensionless modeling and experimental data prediction, and are divided into two types: point source model and solid flame model. Their advantage over CFD models is that they are simple because they do not contain solutions to partial differential equations for fluid flow. The point model assumes that all radiant heat streams of a fire are emitted from a point near the center of the flame. The solid flame model is more detailed. The solid flame shape is determined experimentally, it can be cylindrical or oval, depending on factors such as fuel type and wind speed. Predict radiant heat flux more effectively based on the literature solid flame model.

This paper studies the use of a solid flame model. The flame tilt angle depends on the size of the wind, and the scale line at $\theta = 0^{\circ}$ on the side adjacent to the target tank and the flame is called the meridian, in order to further reduce the effect of the flame on the thermal radiation of the tank, the model of the combination of cone and cylinder is used, and the grid division is shown in Fig. 2.

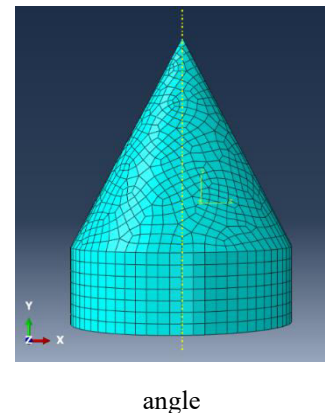
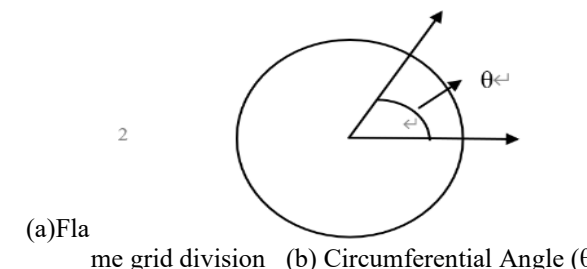


Figure 2

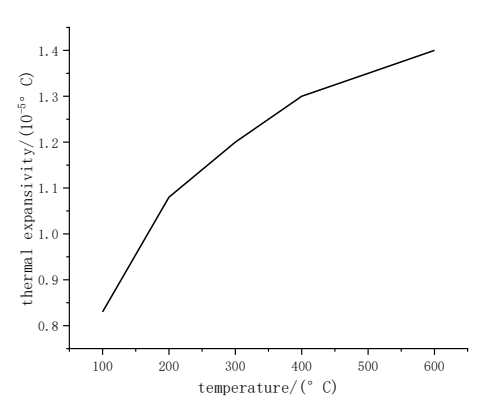
meshing and

Flame geometric



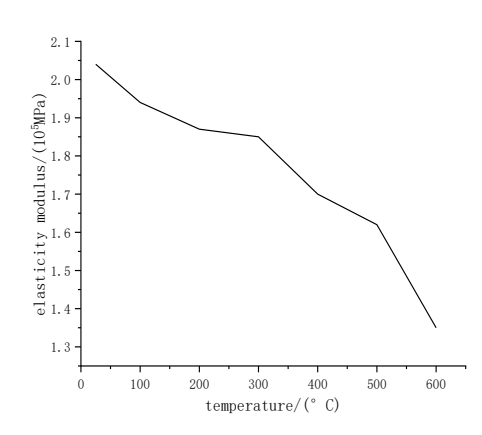
me grid division (b) Circumferential Angle (θ)

Since temperature has an impact on the mechanical properties of Q345 steel, the finite element model adopts the temperature-related mechanical properties parameters of Q345 steel, and the thermal expansion coefficient and elastic



modulus of Q345 steel at different temperatures are shown in Fig. 3. The parameters of Q345 steel are shown in Table 1.

(a) Coefficient of thermal expansion



(b) Elastic modulus

Fig.3 Coefficient of thermal expansion and elastic modulus of Q345 steel

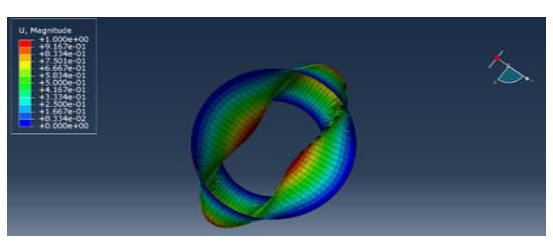
Table 1 Parameters of Q345 steel materials

345 teel	density	Elastic modulus	Poisso n's ratio	Thermal conductivit y	Specific heat capacity
terial amet	7850kg/ m³	210000MPa	0.3	44W/(m)	460J/() kg ⋅ °C

III. EFFECT OF POST-THERMAL BUCKLING BEHAVIOR ON TANK STRUCTURE

In the post-thermal buckling stage, as the temperature rises, there will be a continuous pothole-like deformation near the bottom of the tank and spread to the surrounding area. Buckling occurs again when the transition temperature is reached, and the point mutates again in stress and radial displacement. at the lowest critical temperature θ_L Previously, the stress and radial displacement showed a linear change with temperature, and the point expanded outward by heat and bulged outward (the value is positive). at θ_{L} After that, the deformation of the point gradually changes to an inward depression (the value gradually decreases and eventually becomes negative). This is because the uneven distribution of temperature on the tank wall causes circumferential and axial stresses to be θ_L The circumferential stress on the corresponding region decreases and the axial stress increases [11] at the highest critical temperature during several buckling occurrences θ_H is the boundary line, before which elastic buckling occurs, and then plastic buckling. At this time, the stress increases suddenly and gradually exceeds the yield limit, and the degree of inward depression of the tank wall also intensifies, and plastic deformation occurs at this point and its vicinity. Fig. 4 is a comparison of the tank wall before and after deformation of the plane where the maximum deformation displacement point is located in steady state, and it can be seen that the wall has the maximum radial displacement inward at the same time U_{in} and the maximum radial displacement outward Uout o

Minimum critical temperature θ_L It is the critical point for large deformation of the tank wall, and the occurrence of buckling after heat leads to nonlinear large deformation of the tank body. Under certain conditions, the stress in some areas will exceed the yield limit, that is, there will be both elastic and plastic deformation, and the deformation will intensify with the increase of temperature. The time corresponding to the minimum critical temperature is there fractory time t_L , combine θ_L and θ_H The effects of various factors on the buckling behavior of the tank after heating. The wall thickness can inhibit the deformation of the tank wall to a certain extent, and the first section flame is 10 meters high 800s moment U_{out} and U_{in} The ratio of the difference to the wall thickness t I_u to evaluate the deformation of the tank under the influence of different factors.



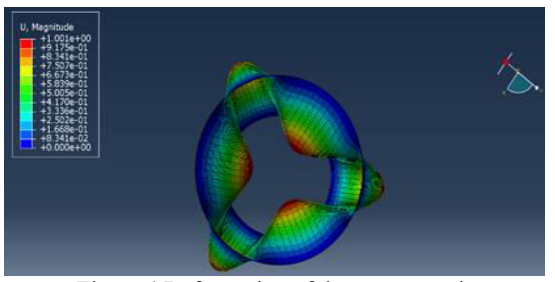


Figure 4 Deformation of the storage tank

IV. INFLUENCE OF DIFFERENT FACTORS ON THE BUCKLING BEHAVIOR OF THE TANK AFTER HEAT

A The effect of flame height

The geometric perspective coefficient is closely related to the shape and size of the flame, so it is necessary to reasonably assume the shape of a pool fire and calculate its flame height. Currently, commonly used solid flame models assume that the pool fire flame is a cylinder that emits a radiant heat flow uniformly through its sides. The height of a solid flame is the average flame length, The average flame length can be calculated using the Heskestad formula:

$$\frac{L_{\rm f}}{D} = -1.02 + 3.7Q^{*2/5} \tag{1}$$

where D is the diameter of the pool fire, m; Q* is the heat release rate with a dimension of 1, which is calculated as:

allated as:
$$Q^* = \frac{x}{\rho_{\infty} c_p T_{\infty} \sqrt{gD} D^2}$$
 (2)

In the formula · X is the heat release rate $X=m_fH$ · m_f is the mass combustion rate · Ethanol is taken 0.029 kg/(s·m²); H It is the heat of combustion · Ethanol is taken 26.8 MJ/kg; ρ_{∞} is the density of air · kg/m³; c_p It is the constant pressure heat capacity of the air ratio · J/(kg·°C); T_{∞} is the air temperature °C; g is gravitational accelerationm/s²

Flame pulsation is an important characteristic phenomenon of turbulent combustion of pool fire, which is a periodic disturbance phenomenon that propagates upward from the bottom of the flame, causing the flame structure to be distorted during the ascent process. Due to the flame pulsation, the surface radiation force of the pool fire flame decreases with the increase of vertical height. If the influence of flame pulsation is ignored, the radiant heat flow predicted by the cylindrical solid flame model is not accurate enough. Therefore, a solid flame model considering flame pulsation (cylindrical-conical solid flame model) can improve the accuracy of predicting radiant heat flow. When the flame pulsates to its lowest, the flame is a cylinder and its height is the continuous flame height (L_c · m) ; When the flame pulsates to its maximum, the flame is a cylindrical-cone combination, with the cylinder height being the continuous flame height and the overall height being the intermittent flame height ($L_i \cdot m$) $\circ L_c$ and L_i the calculation formula is as follows:

$$L_{\rm c} = L_{\rm f} - \frac{\Delta}{2} \tag{3}$$

$$L_{\rm i} = L_{\rm f} + \frac{\Delta}{2} \tag{4}$$

In the formula \cdot Δ is the difference between the intermittent flame height and the continuous flame height \cdot Δ the formula is :

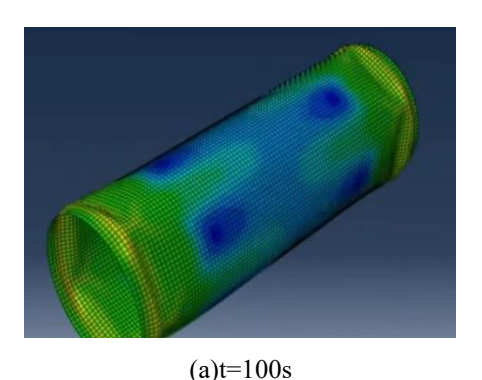
$$\frac{\Delta}{L_f} = Z \sqrt{1 - \frac{z^2}{16}} \tag{5}$$

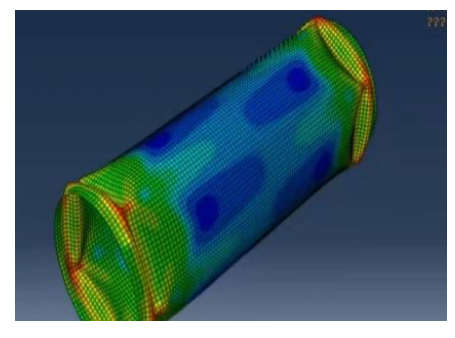
In the formula \cdot Z = C/ L_f /D \cdot The range of coefficient C is:1.20~1.33 (This article is taken 1.27)

After simulation, the flame height directly determines the intensity and distribution range of thermal radiation, which in turn affects the temperature gradient and buckling failure time of the tank wall, and Fig. 5 (a-d) shows the temperature and deformation of the tank at different times. Table 2 shows the critical buckling time of the storage tank under different flame heights, in the windless state. When the flame height \geq the tank height, the flame completely envelops the tank, the thermal radiation efficiency is increased by 2.3 times, and the buckling process is significantly accelerate.

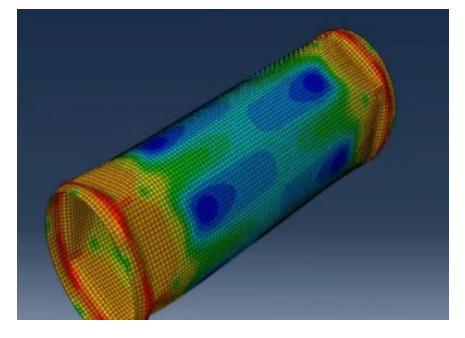
Table 2 Comparison of thermal buckling data at different flame heights

	Hulli	e neignis	
	Не	The	
Fl	at	maxi	Fl
a	flu	mum	ex
m	X	tempe	in
e	of	rature	g ti
he	the	of the	ti
ig	tan	$can\theta_{H}/$	m
ht	k	(°C)	e
(wa		(
m	11		S
)	()
	kw		
	/m		
	2)		
5	15	415	11
	0		00
1	26	674	80
0	0		0
1	33	832	30
5	0		0
2	41	968	18
0	5		0

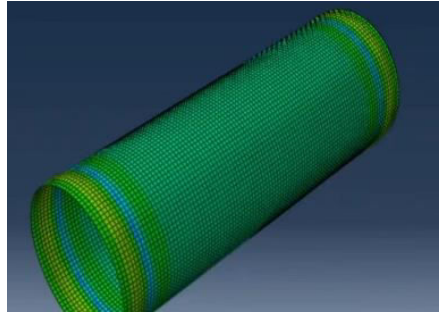




(b)t = 600s



(c)t = 800s



(d)t=1000s

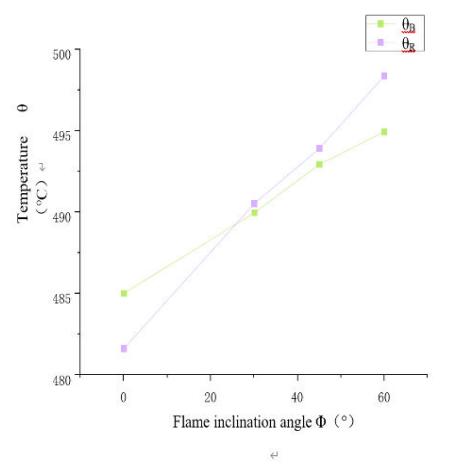
Fig.5 Temperature distribution and deformation of the storage tank under the action of thermal radiation

V. INFLUENCE OF WIND SPEED

During the fire process, the maximum temperature of the tank body $\theta_{\rm E}$ It will be located on the meridian $\theta=0^{\circ}$ At a certain point on the surface of the tank wall. Changes in wind speed can cause the flame to tilt to varying degrees, affecting the distribution of the temperature field of the target tank. The maximum temperature in the top area of the can is $\theta_{\rm R}$.

Figure 5 shows the moment at steady-state $\cdot \theta_{\overline{b}}$ and $\theta_{\overline{R}}$ Angle with flames Φ and the temperature distribution of the target tank. It can be seen that the maximum temperature of the can body $\theta_{\overline{b}}$ Maximum temperature with the top of the tank $\theta_{\overline{R}}$ All increase with the increase of wind speed, but among them $\theta_{\overline{R}}$ The magnitude of change is even more obvious. In addition, the increase of wind speed increases the inclination angle of the flame, the area affected by the flame on the top of the tank gradually expands, and the high-temperature coverage area on the tank body shrinks. At the same time, the convective heat dissipation coefficient of the target tank also increases with the increase of wind speed. Therefore, under different wind speeds, $\theta_{\overline{b}}$ The trend of difference is relatively flat; Due to the increase in the

inclination angle of the flame, the flame is closer to the top



area of the tank, θ_R The trend of change is more significant.

Fig. 5 Maximum temperature and flame inclination

Figure 6 shows the maximum displacement point of the target tank body at a wind speed of 7 m/s I_U Curve in relation to maximum temperature. In the process of temperature rise, the curve is mainly composed of two aspects: one is the inclined section with similar slope, which shows the temperature rise of the tank wall during the post-buckling process; The second is the horizontal line segment, where the temperature remains almost constant, and the tank wall generates a large radial displacement under the action of posterior buckling.

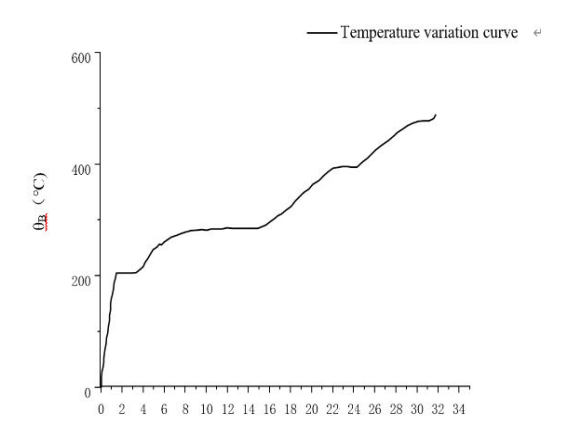
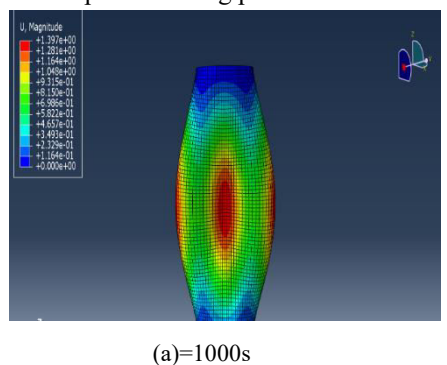


Fig. 6 Balancing path at 7 m/s wind speed

Fig. 7 (a-b) shows the deformation of the tank during the post-buckling process



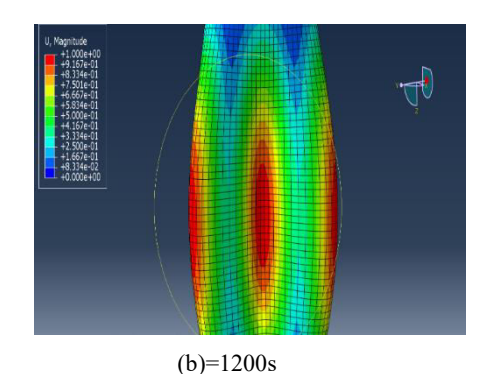


Fig. 7 Temperature distribution of the target tank under the action of thermal radiation

The parameters of the back buckling under different wind speeds and the sum of I_U The statistics are shown in Table 3. Maximum critical temperature θ_H and I_U It is directly proportional to the wind speed \cdot Refractory time t_t and The wind speed is inversely proportional. When the flame inclination angle and convection heat dissipation coefficient increase at the same time, the difference in the maximum temperature is not significant, but the temperature distribution changes. Therefore, the wind speed at θ_L The impact is smaller, while the refractory time is smaller t_t The change is even more obvious. For a wind speed of 7 m/s with a flame inclination of 60 $^{\circ} \cdot I_{U}$ It is 63% higher than that of the windless time, that is, the existence of wind speed causes the radial displacement amplitude of the tank wall to increase, and the degree of unevenness of the wall is aggravated.

Table 3 Relevant parameters corresponding to different wind speeds

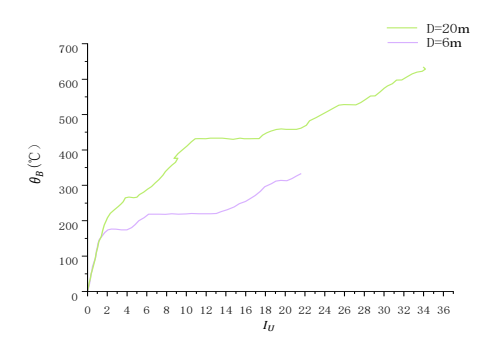
Flame inclination Φ/(°)	$\begin{array}{ll} \text{Minimum} & \text{critical} \\ \text{temperature} & \theta_L/(\square) \end{array}$	Refractory time $t_t/(s)$	$\begin{array}{ll} \text{Maximum} & \text{critical} \\ \text{temperature} & \theta_{\text{H}} / (\square) \end{array}$	l_{u}
0	208	398	450	23.2
30	217	380	465	29.1
45	213	346	468	37.7
60	216	344	477	37.8

VI. INFLUENCE OF DIFFERENT SOURCE TANK DIAMETERS

In most cases, the size of adjacent tanks is inconsistent due to actual production needs and site size. In this section, the diameter of the source tank under the windless condition is taken as the variable, the spacing d=10 m, and the rest of the model parameters remain unchanged. The diameters of the source tank D are 6 m, 10 m, 16 m and 20 m, respectively. When the diameter of the tank increases $\theta_{\overline{a}}$ The temperature of the top area of the tank gradually increases, and the temperature distribution of the target tank along the

Thermal Buckling Study of Empty Thin-Walled Steel Tanks Due To Fire Scenarios

circumference tends to be obvious. As the temperature distribution changes, so does the deformation of the tank walls. Figure 8 gives respectively θ_H The deformation of the target tank at the 2 sample extremes of the source tank.



Pass I_U and θ_B The relationship diagram can be seen · D =20m The deformation of the target tank can be regarded as a continuation of the trend on the basis of deformation at D = 6m, but the subsequent buckling occurs more frequently and more intensely.

Figure 8 Equilibrium path at different spacing

The relevant parameters of the target tank deformation under different tank diameters are shown in Table 4. Minimum critical temperature θ_L and the maximum critical temperature θ_T Proportional to the source tank diameter, Refractory time t_T It is inversely proportional to the diameter of the source tank. With the increase of the diameter of the tank, the increase of the flame radiation area accelerates the temperature rise rate of the target tank. Refractory time t_T shorten. Compared with the largest and smallest source tank diameters in the sample, I_U raised 56%. That is, the degree of depression deformation of the target tank will intensify with the increase of the flame diameter.

Table 4 Relevant parameters corresponding to different source tank diameters

Diameter (m)	$\begin{array}{ll} \mbox{Minimum critical} & \mbox{Refractory} \\ \mbox{temperature} \theta_L / (\square) & \mbox{time} (t) \end{array}$		Maximum critical temperature $\theta_H/(\square)$	Iu
6	192	620	328	21.8
10	208	398	450	23.2
16	239	318	575	27.1
20	269	303	608	33.9

CONCLUSION

In this paper, the effects of flame height, wind speed, and source tank diameter on the post-thermal buckling behavior of the tank were analyzed, and the deformation of the tank and the distribution of corresponding parameters under different factors were obtained, and the following conclusions were drawn.

(1) Minimum critical temperature θ_L It is the critical point of nonlinear large deformation of the tank, and when the temperature exceeds this value, the buckling behavior after heat occurs. In the process of thermal buckling, as the temperature continues to rise, the tank will undergo elastic

deformation and plastic deformation under different environmental conditions, and different degrees of deformation occur in each area of the tank wall.

- (2) The diameters of adjacent storage tanks should not differ too much. During a fire, increased wind speed will shorten the fire resistance time. However, the influence of wind is accidental, and the fire resistance time can be extended by reasonably controlling the rest of the factors t_t , Thus increasing the minimum critical temperature θ_L , It can prevent the occurrence of post thermal buckling behavior \circ
- (3) With the maximum critical temperature θ_H Improvement, The more frequent buckling occurs, the more radial deformation of the tank body will increase, which will cause the tank wall to rupture at a certain time. After the fire resistance time, it is necessary to control the continuous rise of the tank temperature to prevent the escalation and expansion of fire danger.

REFERENCES

- [1] Zhang Qinglin, Zhang Wang, Ren Changxing. Analysis of typical fire cases of oil storage tanks at home and abroad[M]. Tianjin: Tianjin University Press, 2013.
- [2] Yang Guoliang. Research on fire spacing of large crude oil storage tanks based on risk[D].Beijing: China University of Mining and Technology, 2013
- [3] Salahshour S, Fallah F. Elastic collapse of thin long cylindrical shells under external pressure[J]. Thin-Walled Structures, 2018,124: 81-87.
- [4] Pantousa D, Godoy L A. On the mechanics of thermal buckling of oil storage tanks[J]. Thin-Walled Structures, 2019, 145: 106432.
- [5] Li Y, Xu C M, Han S, et al. Failure analysis of weak connection structure of vaulted oil tank under fire condition[J]. CIESCJournal, 2020, 71(7): 3372-3378.
- [6] Santos F D S, Landesmann A. Thermal performance-based analysis of minimum safe distances between fuel storage tanks exposed to fire[J]. Fire Safety Journal, 2014, 69: 57-68.
- [7] RossanaC Jaca, Luis A Godoy, SusanaN Espinosa, et al. International Journal of Pressure Vessels and Piping [J] Thermal post-buckling behavior of oil storage tanks under a nearby fire 2021, 189:104289.
- [8] Li Yunhao, Jiang Juncheng, Yu Yuan, et al. Failure mechanism of fixed vault steel storage tank under the coupling of perforation and thermal radiation[J].CIESC Journal,2021,72(08):4433-4443.
- [9] Hurley M J, Gottuk D, Hall J R, et al. SFPE Hand book of Fire Protection Engineering[M]. New York: Springer, 2016.
- [10] PANTOUSA D, TZAROS K, KEFAKI M A. Thermal buckling behaviour of unstiffened and stiffened fixed-roof tanks under non-uniform heating [J]. Journal of Constructional Steel Research, 2018, 143: 162 179.
- [11] Mo Li, Chen Xing, Chen Chao, et al. Analysis of the buckling behavior of storage tanks after heat under the influence of fire[J].Journal of Safety and Environment,2022,22(06):3075-3081.DOI:10.136371009 -6094.2021.1647.
- [12] Li Shasha, Cui Tie jun. Journal of Safety and Environment[J] Research on the thermal radiation distribution model and regional thermal radiation evolution process of the storage tank liquid tank, 2025,25(3): 910-917.